

SIMULATION MEASUREMENT OF BUNCH EXCITED FIELDS AND ENERGY LOSS
IN VACUUM CHAMBER COMPONENTS AND CAVITIES*

Michael G. Billing, Joseph L. Kirchgessner, and Ronald M. Sundelin**

Abstract

Following the method of Sands and Rees¹, we have developed a two arm comparison apparatus of high sensitivity and good temporal resolution for the measurement of bunch engendered fields. With a relative timing uncertainty of .5 picoseconds the apparatus has demonstrated a sensitivity of .05Ω for the resistive impedance in the presence of a reactive impedance of 4.2Ω for a gaussian shaped bunch of standard deviation 2.1 centimeters. The apparatus is described and results for a typical component are presented. Both energy loss and bunch generated fields are discussed.

Introduction

At Cornell University since January 1976 there has been an on going program of higher mode loss measurements for CESR (Cornell Electron Storage Ring) vacuum chamber components via a double arm comparison apparatus. Based on the method of Sands and Rees¹, a wire along the beam trajectory within the vacuum chamber component carries a current $I_0(t)$ simulating the beam current. The higher mode loss parameter, G, is given by

$$G = 8 \pi \epsilon_0 Z_V \int I_0(t) [I_0(t) - I_m(t)] dt / [\int I_0(t) dt]^2$$

where Z_V is the impedance of the transmission line leading to and from the component piece, and $I_m(t)$ is the current emerging from the component. The average power, P, lost by one beam passing through the given component is related to G by

$$P = G q^2 / 4\pi \epsilon_0 T_{bb}$$

where q is the charge in each bunch and T_{bb} is the time between bunches. For CESR, $P = (408 \text{ W m}) G$. Sands and Rees also calculated the voltage, $V_c(t)$, induced by the beam in the vacuum chamber component:

$$V_c(t) = 2 Z_V [I_0(t) - I_m(t)] = 2 Z_V I_d$$

We have observed that the cavity voltage for all structures, that we have measured, may be described by the following parameterization,

$$V_c(t) = R I_0(t) + L dI_0/dt$$

where R, the resistive impedance, and L, the inductive impedance, can be expressed for a gaussian bunch of standard deviation, σ_z , as

$$R = G \sigma_z Z_V / 2 \sqrt{\pi}$$

$$L = dV_c/dt / d^2 I_0/dt^2$$

where the derivatives are evaluated at the maximum of $I_0(t)$. Another parameter for describing the reactive part of $V_c(t)$ is the reactive impedance, X, where

$$X I_0(t)|_{\max} = L dI_0/dt|_{\max}$$

Description of the Method and Apparatus

In a single arm measurement I_0 is measured using a reference piece of vacuum chamber. I_m is then measured at the output of the piece in question. From recordings of these signals the difference signal is computed. In the double arm method the difference is taken directly in the hardware of the apparatus, leaving only small corrections of the differences in the two arms to be made later. Since the results of the subtractions are very sensitive to the relative timing of the two signals, the double arm method can measure smaller losses than can reliably be done with a single arm method.

A schematic of the apparatus is seen in figure 1. The simulated beam pulse originates from the pulser² which produces a nearly gaussian pulse of full width at half maximum (FWHM) of 140 ps. Following the pulser are two directional couplers, one for the scope trigger and the other for a precursor timing signal (to be discussed below), and a 75 ns high frequency delay line which is necessary for the scope pre-trigger. At this point a gaussian pulse of approximately 4 V and FWHM = 160 ps is applied in the double arm apparatus. Matched splitters T1 and T2 are needed for splitting up the signal and summing the resultant waveforms respectively. Phase shifters P1 through P4 are used for line length adjustments, while attenuators A1 through A4 are for balancing. Transition horns H1 through H4 match 50Ω transmission lines to the vacuum chamber cross section and the impedance desired in the measurement, typically 157Ω. The compensation arm contains the wide band pulse inverter, while the measurement arm has a pulse non-inverter for matching purposes. Finally, either arm may be viewed independently or jointly via coaxial switches S1 and S2 allowing four different possible signals to emerge from the double arm apparatus. The signal, that has been chosen, passes through another directional coupler, which impresses the precursor signal on the waveform. The resultant waveform is detected by a sampling oscilloscope, whose sampling timing sweep is driven by a ramp signal from a digital signal averager. The signal averager digitizes the vertical amplifier output from the oscilloscope to increase the signal-to-noise ratio. The contents of the memory of the averager is transmitted to a PDP-10 computer for analysis.

The mechanical arrangement of the RF components of the apparatus is crucial for stability and repeatability. This is accomplished by using airline and semi-rigid coaxial transmission line, 20 cm or longer between every RF component to minimize the problem of reflections, and by mounting all components to a rigid structure. Since it is necessary to change vacuum chamber pieces between H1 and H3, and H2 and H4, all components from the pulser to H1 and H2 are attached to a separate cart, which is free to slide relative to the main supporting frame.

* Work supported by the National Science Foundation.

** Laboratory of Nuclear Studies, Cornell University, Ithaca, New York 14853.

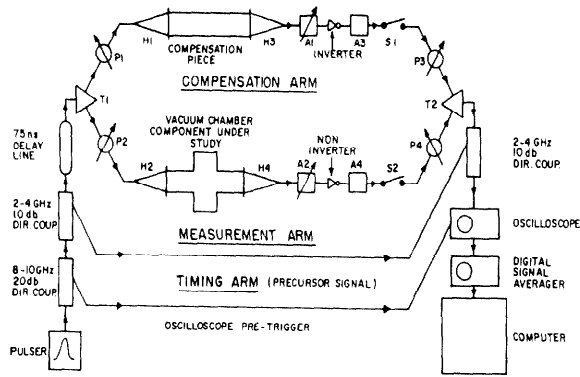


Figure 1. Schematic of the Double Arm Apparatus

Typical Measurement and Analysis

A typical measurement proceeds as follows. A nulling piece is placed in the measurement arm, and the signals from the compensation arm, the measurement arm, and their difference labelled respectively I_{un} , I_0 , and I_n would be recorded. Next the vacuum chamber component of interest is exchanged for the nulling piece and the analogous signals recorded; this time the signals are labelled I_{un} , I_m , and I_a . Due to reflections from the transmission line elements in the apparatus, it is not possible to produce a null signal identically zero, thus I_n must be subtracted from I_a in order to obtain the "true" difference signal, I_d .

Because the waveforms are detected on a digital signal averager that uses a sampling oscilloscope as a fast signal stretcher, the averaged signal may slew randomly in time. To determine I_d and G , the relative timing of I_0 , I_a and I_n (hereafter referred to as timing) must be obtained accurately, requiring that every waveform be impressed with the same timing fiducial which is then employed to correct the relative temporal displacements of the waveforms. This fiducial signal is generated from the input pulse itself via a directional coupler and is placed in front of all waveforms as a precursor pulse. Since the precursor signal does not pass through either the compensation arm or the measurement arm, it is present when both switches are open and this output is labelled I_z .

For the standard double arm measurement analysis on the PDP-10 the program uses only I_0 , I_a , I_n , and I_z . First each waveform is separated into the precursor part and the signal part, and the relative timing determined. To calculate the relative timing between two signals their precursors are subtracted after shifting the signals back and forth in time relative to one another. The proper time shift is found when the difference most nearly fits a straight baseline. (In order to allow for the front porch on I_0 , this baseline is permitted to have a slope.) After determining the relative timing of the waveforms the average I_z without the precursor is used as the baseline for I_0 . At this point the program calculates the double arm difference signal, $I_{d;D}$, and the higher mode loss parameter, G_D . The same analysis can be used to calculate $I_{d;S}$ and G_S for an equivalent single

arm measurement (using only waveforms derived from the measurement arm) by simply substituting I_0 for I_a and I_m for I_n .

Measurement Uncertainties

The measurement uncertainties for higher mode measurements depend on many variables, including the shape of $V_c(t)$, i.e., the relative amounts of inductive to resistive part of the cavity voltage, the timing uncertainty, the signal-to-noise ratio, and the apparatus frequency response in relation to the important bunch frequencies. As an example, the measurement of the uncertainties for a typical vacuum chamber component is presented.

For this measurement the fast kicker metallized ceramic vacuum chamber for CESR with its attached bellows (figure 2) was used. This particular piece was chosen for its moderate G (approx. 1.5 m^{-1}) and the fact that the cavity voltage shows the presence of an inductive as well as resistive component. The measurement consisted of several measurements of the ceramic and several nulls for a gaussian pulse of $\sigma_z = 2.1 \text{ cm}$. Examples of waveforms are found in figure 3. It is possible to use the waveform itself to calculate the required time shift between two subsequent null signals. Thus the timing uncertainty can be measured by first using the precursor signal to calculate the time shift of the waveforms and then using the waveform itself to calculate any additional time shift needed. A histogram of TSHIFT, the additional time shift to align the null signals, is given in figure 4 with the binning being .25 ps. The histogram of TSHIFT implies that the signal averaging and data analysis determine the relative timing of the null signals to within .5 ps.

Results from this set of data are histogrammed for both double arm and single arm calculations of G (shown respectively in figures 5 and 6). The binning for figure 5 is $.01 \text{ m}^{-1}$ and for figure 6 is $.2 \text{ m}^{-1}$, and the results may be summarized as

$$G_D = 1.40 \pm .05 \text{ m}^{-1}$$

$$G_S = 1.70 \pm .2 \text{ m}^{-1}$$

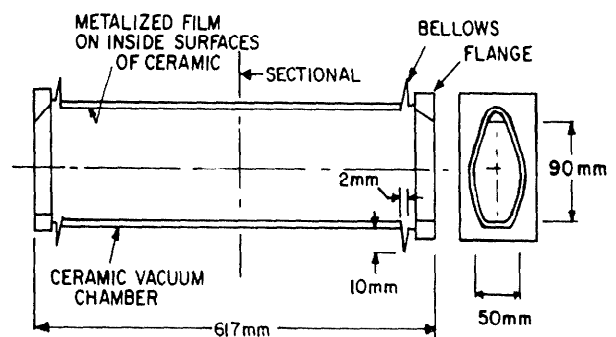


Figure 2. Metallized Ceramic Vacuum Chamber.

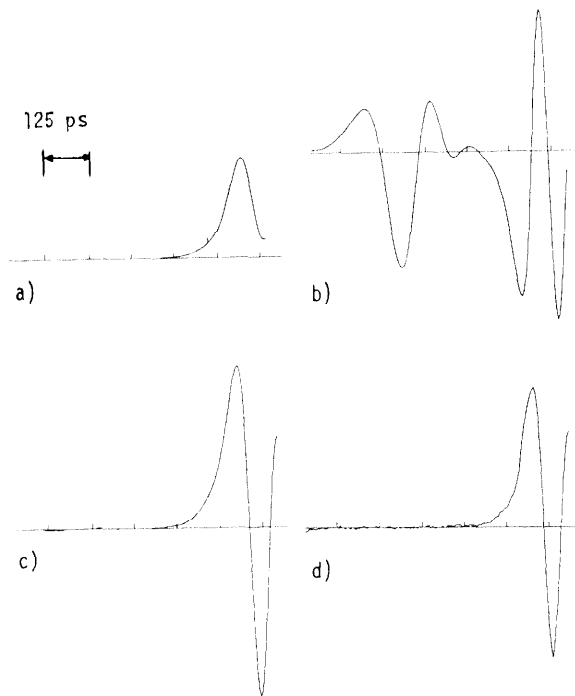


Figure 3. Typical Waveforms a) I_0 , b) I_n , c) $I_{d;D}$, d) $I_{d;S}$. (Vertical scale is in relative units with the scale for I_0 , 50 times the others.)

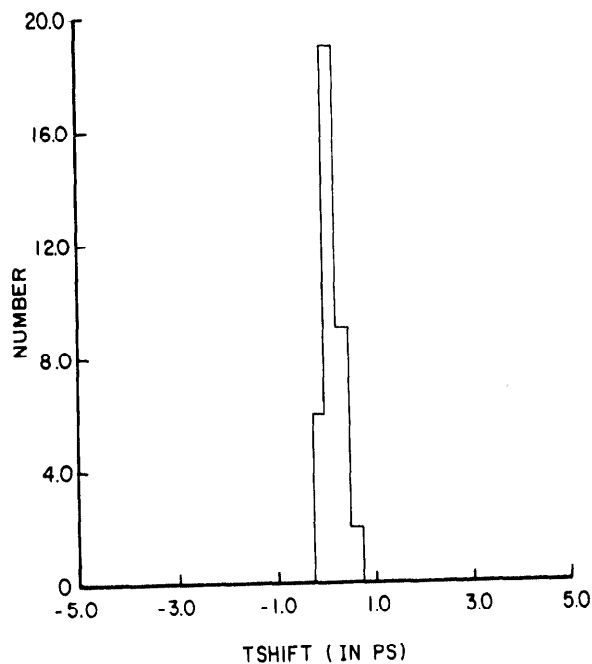


Figure 4. Histogram of Timing Uncertainty.

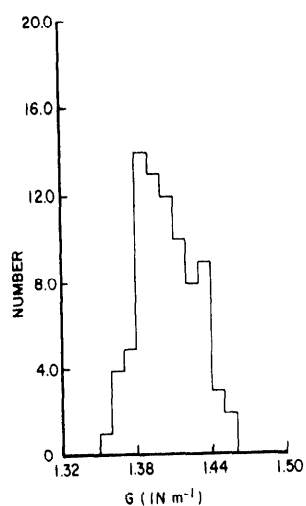


Fig. 5 Histogram of G_D .

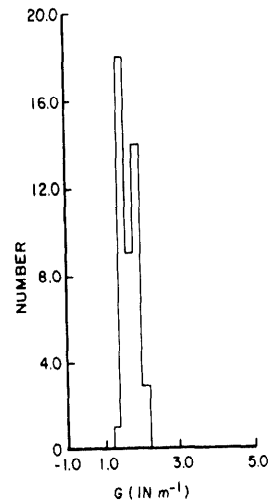


Fig. 6 Histogram of G_S .

The uncertainties in G are caused by timing uncertainties and zero baseline uncertainties produced by noise in the signals.

The peak value of V_c scaled from the measurement to 1.5×10^{12} particles_c in a 2.1 cm bunch is

$$V_c = 14.3 \pm .2 \text{ KV} \quad \text{double arm}$$

$$V_c = 14.5 \pm 3.8 \text{ KV} \quad \text{single arm}$$

These uncertainties in V_c are caused by residual common mode signals due to timing inaccuracies. The ceramic measurement yields the following results for the cavity voltage parameters describing earlier

$$R = 1.28 \pm .05 \Omega$$

$$L = .48 \pm .05 \text{ nH}$$

$$X = 4.2 \pm .4 \Omega.$$

References

- 1) M. Sands and J. Rees, SLAC Report PEP-95 (1974).
- 2) The pulser is on loan from Jens Peters, DESY, Hamburg, Germany.